POLITECNICO DI TORINO
Repository ISTITUZIONALE

Low-Frequency Modal Extrapolation and Regularization for Full-Bandwidth Macromodeling of Electromagnetic Structures

Original
Low-Frequency Modal Extrapolation and Regularization for Full-Bandwidth Macromodeling of Electromagnetic Structures / De Stefano, M.; Grivet-Talocia, S.; Wendt, T.; Yang, C.; Schuster, C.. - ELETTRONICO. - (2022), pp. 1-4. ((Intervento presentato al convegno 2022 IEEE 26th Workshop on Signal and Power Integrity (SPI) tenutosi a Siegen, Germany nel 22-25 May 2022 [10.1109/SPI54345.2022.9874931].

Availability:
This version is available at: 11583/2971248 since: 2022-09-13T06:13:20Z

Publisher:
IEEE

Published
DOI:10.1109/SPI54345.2022.9874931

Terms of use:
openAccess

This article is made available under terms and conditions as specified in the corresponding bibliographic description in the repository

Publisher copyright
IEEE postprint/Author's Accepted Manuscript

©2022 IEEE. Personal use of this material is permitted. Permission from IEEE must be obtained for all other uses, in any current or future media, including reprinting/republishing this material for advertising or promotional purposes, creating new collecting works, for resale or lists, or reuse of any copyrighted component of this work in other works.

(Article begins on next page)

29 November 2022

Low-Frequency Modal Extrapolation and Regularization for Full-Bandwidth Macromodeling of Electromagnetic Structures

M. De Stefano*, S. Grivet-Talocia*, T. Wendt†, C. Yang†, C. Schuster†
*Dept. Electronics and Telecommunications, Politecnico di Torino, Italy
†Institut für Theoretische Elektrotechnik, Hamburg University of Technology (TUHH), Hamburg, Germany

***Abstract*—This paper provides a novel strategy for the extrapolation and regularization of low frequency data of low-loss or lossless structures, based on asymptotic modal trajectories. The proposed data-driven strategy is intended as a fundamental preprocessing step to obtain a full-bandwidth reliable macromodel to be used in transient simulations, providing full control of the low-frequency and DC behavior of the system.**

I. Introduction

This paper presents a data conditioning strategy for enhancing the generation of rational macromodels of low-loss electromagnetic structures characterized by sampled frequency responses. The application we have in mind arises from the characterization of nonlinearly loaded shielding enclosures [1], which due to the presence of nonlinear elements requires an aggressive accuracy in all modeling steps, in particular including low-frequency and the zero-frequency (DC) point. The procedure that we propose is however general and applicable to low-frequency extrapolation of data for a wide range of applications, including Signal and Power Integrity, where transient analysis of large electromagnetic systems with nonlinear terminations is a common task.

This paper draws the main idea of Analytic Extension of Eigenvalues [2], which performs a physics-based extrapolation based on an asymptotic continuation of eigenvalue trajectories, in a form that is compatible with a low-frequency lumped circuit representation. We provide a number of generalizations, motivated by our objective of generating reliable macromodels over an extended frequency band, including the DC point. This problem is highly relevant due to the following issues.

- Common frequency-domain field solvers based on Method of Moments (MoM) or Finite Elements (FE) cannot provide accurate responses below a critical frequency $f_{\min}$. Some kind of low-frequency extrapolation is therefore required to provide training data samples to the macromodeling engine. It is well known that missing frequency samples especially at low frequency usually lead to inaccurate and physically inconsistent macromodels.
- Many low-frequency extrapolation schemes have been presented to deal with this problem (see e.g. [3] and references therein). These usually assume a regular DC behavior, therefore most applications apply such schemes to scattering responses, which are well-behaved and bounded at DC. However, when the structure under investigation is low-loss or in the limit lossless (an assumption that is often used by field solvers), the eigenvalues of the scattering matrix become very close to one (equal to one) in magnitude at DC. This implies that conversion to impedance or admittance representations, or equivalently simulating the model with a (transient) circuit solver using low/high impedance or reactive terminations may lead to extremely inaccurate results, due to the model sensitivity [4] and error magnification [5].
- A DC regularization is often used to prevent such sensitivity issues, either explicitly [6] or implicitly (e.g. several SPICE solvers regularize the underlying Modified Nodal system by adding a small conductance to every node, in order to improve convergence during operating point evaluation). Unfortunately, low-frequency DC extrapolation of frequency data from a field solver combined with an explicit regularization at DC (or even with DC data from a dedicated static solver) may lead to data discontinuities and abrupt transitions, which further challenges the macromodel generation, leading to spurious poles and dramatic passivity violations.

This paper describes an algorithm that performs a simultaneous regularization and extrapolation, and provides a low frequency extrapolation that smoothly joins a physics-based DC response to the field solver responses. The algorithm is even applicable to those limit cases of lossless structures that have a singular DC behavior (a DC pole) for both impedance and admittance, which are particularly challenging for macromodeling applications. The working test case that we use to illustrate the proposed algorithm follows in this class of problems.

II. Motivation: a Case Study

Figure 1 depicts a shielding enclosure with an aperture, where a number of ports $P = p^2$ are defined on a regular $p \times p$ series/parallel grid. The enclosure is part of an energy-selective shield, obtained by loading the ports with nonlinear elements (back-to-back diode pairs). For an overview of energy-selective shielding see [7], in particular [1], [8], where the dependence of the shielding effectiveness on the amplitude/energy of the impinging fields is documented. The

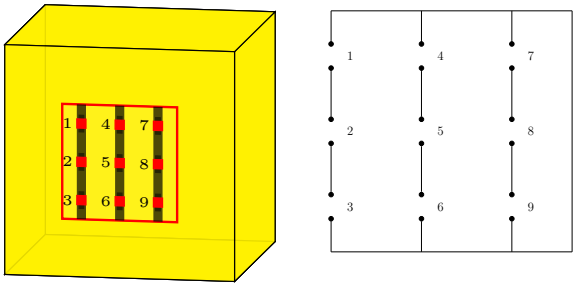

Fig. 1. Left: A shielding box with $P = 9$ ports, arranged in $p = 3$ parallel branches, each including p vertically aligned (series) ports. Right: DC equivalent circuit, where the return path through the enclosure is represented by the short circuit on the right.

shield blocks high-amplitude potentially dangerous fields and is almost transparent to low-amplitude fields.

Our final objective is transient simulation of the loaded structure for time-domain shielding verification, using an approach that constructs a reduced-order macromodel for the unloaded structure starting from field solver data, realizes the macromodel as a low complexity behavioral netlist, and performs transient analysis after connecting nonlinear loads at all ports. See [9] for a complete description of this flow.

As starting data to construct the macromodel of the unloaded shield, we consider port responses computed by a MoM solver [10], available at K frequency points in the frequency range $[f_{\min}, f_{\max}]$, where due to intrinsic limitations in the solver formulation $f_{\min} > 0$. The material used to model the box is a Perfect Electric Conductor (PEC), so that a physics-based zero-frequency model is readily obtained as in Fig. 1. Under these conditions, both the impedance and the admittance matrices become ill-defined when the frequency vanishes, since they both have one dominant DC pole. This behavior is confirmed by the top panel of Fig. 2, which depicts the frequency-dependent admittance matrix elements (magnitude) for $f \geq f_{\min}$ from the MoM solver. A similar behavior holds for the impedance matrix elements.

Our objective is to provide a smooth extrapolation to DC in order to build a physically-consistent model at low frequencies, and at the same time regularize the data hence the model in order to avoid the DC pole. The latter would make any transient simulation using the model unreliable due to lack of asymptotic stability.

III. Regularization and Extrapolation

A. Regularization

Since both impedance $\mathbf{Z}(s)$ and admittance $\mathbf{Y}(s)$ matrices of the structure are singular (do not exist) at DC, we perturb the topology by adding regularization resistors, so that both representations become nonsingular. In particular, we regularize $\mathbf{Z}(s)$ by adding a large *shunt* resistance R to each port, and then we regularize $\mathbf{Y}(s)$ by adding a small *series* resistance r to each port. The resulting regularized

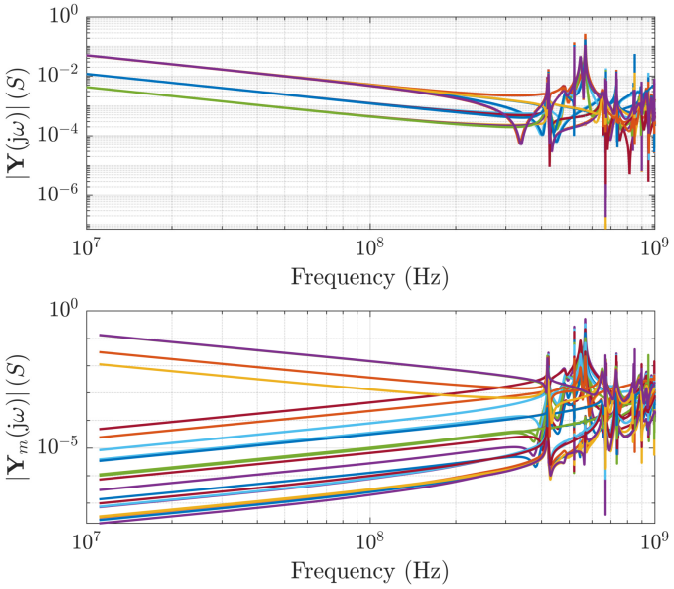

Fig. 2. Admittance responses of the shielding enclosure of Fig. 1. Top: data from the MoM solver; bottom: projection onto DC asymptotic modes.

DC equivalent circuit is non-singular for any immittance representation and is described by the DC admittance matrix

$$\mathbf{Y}(s=0) = \mathbf{Y}_0 = \mathbb{I}_p \otimes \mathbf{Y}_p, \quad \mathbf{Y}_p = \frac{(p\,r\,\mathbb{I}_p + R\boldsymbol{u}\boldsymbol{u}^{\mathsf{T}})}{p\,r(R+r)} \quad (1)$$

where $\boldsymbol{u}^{\mathsf{T}} = [1, \cdots, 1]$, $\boldsymbol{u} \in \mathbb{R}^p$, $\mathbb{I}_p$ is the size-p identity matrix, and $\otimes$ is the Kronecker product. A compatible regularization of the data from the field solver can be easily applied, in order to make the solver responses compatible with the DC response (1). This is achieved by converting the solver responses to admittance, adding R^{-1} to the main diagonal, converting to impedance, and finally adding r again to the main diagonal. This operation is well defined at any frequency $f \in [f_{\min}, f_{\max}]$ since the DC point is missing from the solver data.

B. Low frequency extraction

An extrapolation of the frequency responses below the first available frequency point from the solver is not trivial. Since the raw (before regularization) impedance and admittance matrices $\mathbf{Y}(\mathrm{j}\omega) \to \infty$ and $\mathbf{Z}(\mathrm{j}\omega) \to \infty$ for $\omega = 2\pi f \to 0$, we know that each of these two matrices has a set of eigenvalues that tends to zero and a set of eigenvalues that approaches ∞ at low frequency. The vanishing admittance eigenvalues correspond to the exploding impedance eigenvalues, and vice versa. This implies that *both* small and large eigenvalues must be accurately modeled. This is impossible when operating in the physical domain, since small eigenvalues are shaded by large eigenvalues. Conversion to the modal domain is inevitable in order to separate small from large eigenvalues. Note that, with reference to the impedance representation, small (large) eigenvalues correspond to inductive (capacitive) modes at low frequency.

Differently from [2], which adopts a data-based eigendecomposition, we define the modes based on the regularized DC circuit. This choice is motivated by two facts: first, the numerical approximations from the solver lead to an error term in the computed frequency responses, so that the eigenvectors computed at any finite frequency may be imprecise and do not generally correspond to the eigenvectors at DC. Second, such eigenvectors are generally complex-valued, and in order to preserve the causality of the extrapolated responses we need purely real modal transformations, a fact that has been extensively discussed in [11].

We start with the eigenvalue decomposition of the regularized DC admittance matrix $\mathbf{Y}_0$ in (1) as

$$\mathbf{Y}_0 = \mathbf{Q}\mathbf{\Lambda}_0\mathbf{Q}^\mathsf{T}, \quad \mathbf{\Lambda}_0 = \mathbf{Q}^\mathsf{T}\mathbf{Y}_0\mathbf{Q} = \begin{bmatrix} \frac{1}{R'}\mathbb{I}_c & \mathbf{0} \\ \mathbf{0} & \frac{1}{r}\mathbb{I}_\ell \end{bmatrix} \tag{2}$$

where $R' = R + r$, showing that the eigenvalue $1/R'$ has multiplicity $c = p(p-1)$ and the eigenvalue $1/r$ has multiplicity $\ell = p$. Since $\mathbf{Y}_0$ is symmetric, the modal matrix $\mathbf{Q} = \begin{bmatrix}\mathbf{Q}_p & \mathbf{Q}_s\end{bmatrix}$ is orthogonal, so that $\mathbf{Q}_s^\mathsf{T}\mathbf{Q}_s = \mathbb{I}_\ell$, $\mathbf{Q}_p^\mathsf{T}\mathbf{Q}_p = \mathbb{I}_c$, and $\mathbf{Q}_p^\mathsf{T}\mathbf{Q}_s = \mathbf{0}$. We can thus write

$$\mathbf{Y}_0 = \frac{1}{R'}\mathbf{Q}_p\mathbf{Q}_p^\mathsf{T} + \frac{1}{r}\mathbf{Q}_s\mathbf{Q}_s^\mathsf{T}. \tag{3}$$

Note that ℓ and c indicate the number of inductive and capacitive modes, respectively.

The matrix $\mathbf{Q}$ storing as columns the DC asymptotic modes is then used to project onto the corresponding modal domain the data from the field solver. Since $\mathbf{Q}$ is constant and orthogonal, the following similarity (congruence) transformation explicitly preserves the causality and the passivity of the data upon modal conversion. We compute for all frequency samples

$$\mathbf{Y}_m(\mathrm{j}\omega_k) = \mathbf{Q}^\mathsf{T}\mathbf{Y}(\mathrm{j}\omega_k)\mathbf{Q}\,, \quad k = 1, \cdots, K. \tag{4}$$

The results of this transformation are depicted in the bottom panel of Fig. 2, confirming that the various modal impedance and admittance elements are either directly or inversely proportional to frequency. Collecting coefficients associated to powers of frequency in the low frequency (LF) range we have

$$\mathbf{Y}_m(\mathrm{j}\omega) \approx \frac{1}{\mathrm{j}\omega}\mathbf{\Gamma}_m + \mathrm{j}\omega\mathbf{C}_m = \begin{bmatrix} \mathrm{j}\omega\widetilde{\mathbf{C}} & \mathrm{j}\omega\mathbf{X} \\ \mathrm{j}\omega\mathbf{X}^\mathsf{T} & \frac{1}{\mathrm{j}\omega}\widetilde{\mathbf{\Gamma}} \end{bmatrix} \tag{5}$$

where $\mathbf{\Gamma}_m$ and $\mathbf{C}_m$ are constant matrices having the property that for each element i, j such that $(\mathbf{\Gamma}_m)_{ij} \neq 0$ the corresponding element $(\mathbf{C}_m)_{ij} = 0$, and vice versa. The block structure of the dominant terms is also detailed in (5). The nonvanishing elements of the constant matrices $\mathbf{\Gamma}_m$ and $\mathbf{C}_m$ are determined though an element-wise regression using few frequency samples from the modal data in a suitable band $(f_{\min}, f_0)$ where modal responses behave asymptotically, as in the bottom panel of Fig. 2. Availability of such frequency interval is a prerequisite for proposed method. The expression (5) is used to extrapolate the data for $f \in (0, f_{\min})$, and the result is regularized in the modal domain, following the procedure discussed next.

C. Regularization in the modal domain

The structure of the admittance matrix in the asymptotic modal domain (5) is now exploited to perform a regularization process similar to Section III-A, directly in the modal domain. The main advantage of this approach is that only the individual modes that are responsible for the singularity of a given (modal) matrix block representation are regularized, leaving the other modes (blocks) unperturbed. The result is a numerically robust procedure that can be used to regularize and extrapolate our dataset smoothly to DC.

Noting from (5) that the capacitive block $\mathrm{j}\omega\widetilde{\mathbf{C}}$ is the responsible for the singularity of $\mathbf{Y}_m(\mathrm{j}\omega)$ for $\omega \to 0$, we first regularize only this block

$$\widehat{\mathbf{Y}}_m(\mathrm{j}\omega) = \mathbf{Y}_m(\mathrm{j}\omega) + \begin{bmatrix} \frac{1}{R'}\mathbb{I}_c & \mathbf{0} \\ \mathbf{0} & \mathbf{0} \end{bmatrix} \tag{6}$$

The resulting matrix is nonsingular at any finite frequency and can be inverted. The result is then regularized in its inductive block as

$$\breve{\mathbf{Z}}_m(\mathrm{j}\omega) = \widehat{\mathbf{Y}}_m(\mathrm{j}\omega)^{-1} + \begin{bmatrix} \mathbf{0} & \mathbf{0} \\ \mathbf{0} & r\mathbb{I}_\ell \end{bmatrix} = \begin{bmatrix} R'\,\mathbb{I}_c + \star_1 & \star_2 \\ \star_2 & r\,\mathbb{I}_\ell + \star_1 \end{bmatrix}$$

where the symbol $\star_\nu$ denotes a frequency-dependent matrix with leading order $(\mathrm{j}\omega)^\nu$ for $\omega \to 0$. We see that the regularized modal impedance matrix $\breve{\mathbf{Z}}_m(\mathrm{j}\omega)$ is compatible with the inverse of the DC modal admittance matrix derived in (3), thus providing a smooth interpolation to DC. Returning to the physical domain through inverse modal transformation leads to the final regularized response

$$\breve{\mathbf{Z}}(\mathrm{j}\omega) = \mathbf{Q}\,\breve{\mathbf{Z}}_m(\mathrm{j}\omega)\,\mathbf{Q}^\mathsf{T}, \tag{7}$$

which is nonsingular and bounded at any frequency, including DC, and which is used to extrapolate the regularized solver data in the LF range.

IV. Results

The effectiveness of the proposed data preprocessing is now illustrated on a test case. We consider a shielding enclosure similar to Fig. 1, with $P = 25$ ports regularly spread over a 5×5 grid throughout a square aperture. The adopted MoM solver was used to generate scattering responses, which are sufficiently accurate starting from $f_{\min} = 10$ MHz. The proposed extrapolation and regularization procedure was applied to fill the gap from 100 Hz to $f_{\min}$, using the interval $(f_{\min}, f_0)$ with $f_0 = 20$ MHz to compute the extrapolation coefficients of (5) via regression, while providing a reliable DC point for the subsequent macromodeling process. The resistance values used for regularization ($r = 0.1\ \Omega$, $R = 100\ \mathrm{M}\Omega$) are such that the perturbation of the high-frequency MoM data is negligible, see Fig. 3a.

Two macromodels are constructed. The first is built by fitting the original MoM data with the added DC point only, without any low-frequency extrapolation. The second uses instead the regularized and extrapolated frequency samples. Both models are constructed using responses in the scattering representation. However, model-data comparison is illustrated

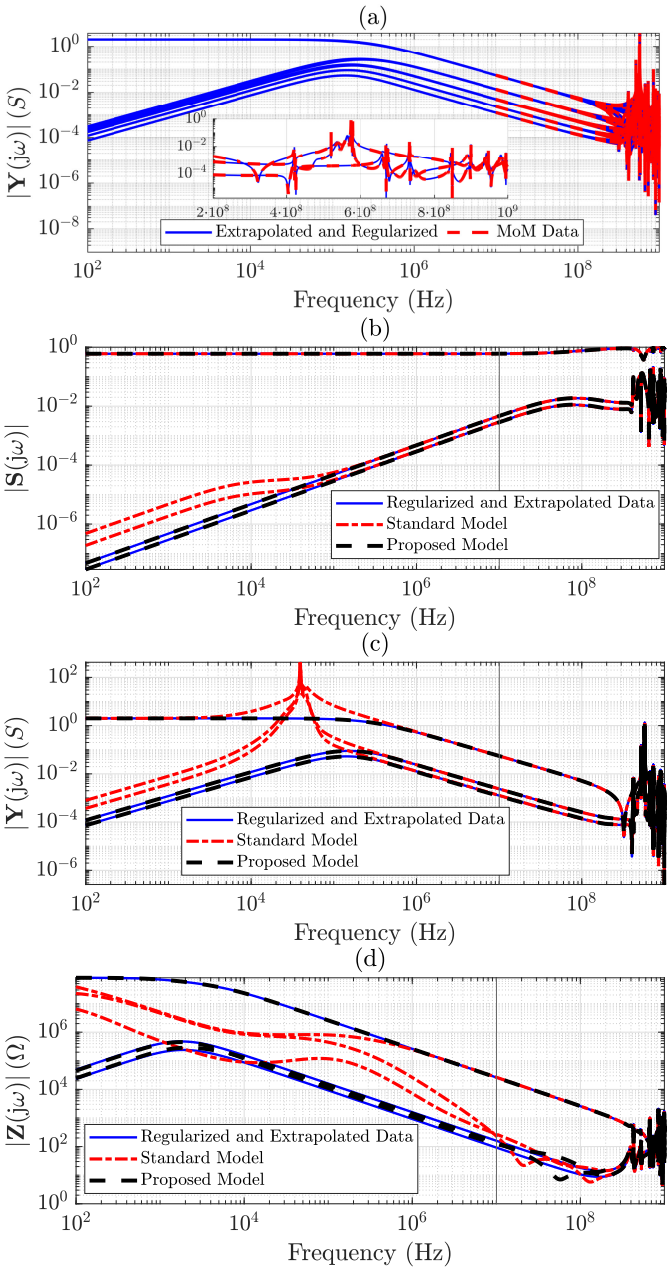

Fig. 3. Modeling a 25-port shielding enclosure: (a) admittance parameters from MoM solver and computed regularized extrapolation (inset: detail on high-frequency); (b) validation of standard and proposed macromodel responses in scattering representation; (c) and (d) same as (b), but in admittance and impedance representation.

for the three main input-output representations: scattering (Fig. 3b), admittance (Fig. 3c) and impedance (Fig. 3d), where the latter two are obtained by basic conversion as postprocessing. Impedance and admittance responses indicate the model behavior with its ports loaded by high-impedance (open) and low-impedance (shorted) terminations, respectively.

The results confirm that all models are accurate in the high-frequency region where MoM data are available, for all three representations. However, the model behavior at low frequency is highly sensitive for both impedance and admittance representations. The model constructed on unprocessed raw data appears to be physically inconsistent in the LF range. Conversely, the model constructed using regularized and extrapolated data provides a consistent behavior even in the LF range, by smoothly converging to the expected DC responses, and by retaining excellent accuracy in all three representations over the full band. These results imply that the model will behave consistently, independently on the terminations used to load the structure, and in particular in presence of nonlinear terminations as assumed by the energy-selective shielding application at hand.

V. Conclusion

A simple data conditioning algorithm was presented, which is able to smoothly extend frequency responses from a field solver at low frequencies down to the DC point. This procedure is able to significantly improve the low frequency behavior of behavioral macromodels, which exhibit a major accuracy improvement and a drastically reduced sensitivity to terminations. The procedure was illustrated on a test case related to energy-selective shielding, but the main algorithm is general and can be applied in principle to any signal/power interconnect structure.

References

[1] C. Yang, P. Liu, and X. Huang, "A novel method of energy selective surface for adaptive HPM/EMP protection," *IEEE Antennas Wirel. Propag. Lett.*, vol. 12, pp. 112–115, 2013.

[2] H. Li, J.-M. Jin, D. R. Jachowski, and R. B. Hammond, "Fast frequency sweep analysis of passive miniature rf circuits based on analytic extension of eigenvalues," *IEEE Transactions on Microwave Theory and Techniques*, vol. 69, no. 1, pp. 4–14, 2021.

[3] J. Cho, J. Ahn, J. Kim, J. Park, Y. Shin, K. Kim, J. Choi, and S. Ahn, "Low- and high-frequency extrapolation of band-limited frequency responses to extract delay causal time responses," *IEEE Transactions on Electromagnetic Compatibility*, vol. 63, no. 3, pp. 888–901, 2021.

[4] A. Ubolli, S. Grivet-Talocia, M. Bandinu, and A. Chinea, "Sensitivity-based weighting for passivity enforcement of linear macromodels in power integrity applications," in *DATE 2014 - Design, Automation and Test in Europe, Dresden, Germany*, March 24–28, 2014, pp. 1–6.

[5] B. Gustavsen and C. Heitz, "Modal vector fitting: A tool for generating rational models of high accuracy with arbitrary terminal conditions," *Advanced Packaging, IEEE Transactions on*, vol. 31, no. 4, pp. 664–672, nov. 2008.

[6] S. Grivet-Talocia and F. Canavero, "Dc-compliant macromodels based on the method of characteristics for frequency-dependent transmission lines," in *2006 1st Electronic Systemintegration Technology Conference*, vol. 1, 2006, pp. 56–61.

[7] G. V. Eleftheriades, "Protecting the weak from the strong," *Nature*, vol. 505, no. 7484, pp. 490–491, 2014. [Online]. Available: https://doi.org/10.1038/nature12852

[8] T. Wendt, C. Yang, H. D. Brüns, S. Grivet-Talocia, and C. Schuster, "A macromodeling-based hybrid method for the computation of transient electromagnetic fields scattered by nonlinearly loaded metal structures," *IEEE Transactions on Electromagnetic Compatibility*, vol. 62, no. 4, pp. 1098–1110, Aug 2020.

[9] T. Wendt, C. Yang, S. Grivet-Talocia, and C. Schuster, "Numerical complexity study of solving hybrid multiport field-circuit problems for diode grids," in *International Conference on Electromagnetics in Advanced Applications (ICEAA 2019)*, September 2019.

[10] "CONCEPT-II, 2019." [Online]. Available: http://www.tet.tuhh.de/concept/

[11] B. Gustavsen, "Rational modeling of multiport systems via a symmetry and passivity preserving mode-revealing transformation," *IEEE Transactions on Power Delivery*, vol. 29, no. 1, pp. 199–206, 2014.